Neoplasia • Vol. 1, No. 6, December 1999, pp. 498–507 

Available On-line at http://www.neoplasia.org

# Novel Suicide Ligands of Tubulin Arrest Cancer Cells in S-Phase[1]

*Ashley Davis*[2], Jian-Dong Jiang*[2], Kim M. Middleton*, Yue Wang*, Imre Weisz*, Yi-He Ling‡ and J. George Bekesi**

*Cytoskeleton Inc., 1650 Fillmore Street, #240, Denver, CO 80206; *T.J. Martell Laboratory for Leukemia, Cancer and AIDS Research, Department of Medicine, Mount Sinai School of Medicine, New York, NY 10029; ‡Kaplan Comprehensive Cancer Center, New York University Medical School, New York, NY 10016

**Abstract**

**It is presently accepted that the mechanism of action for all anti-tumor tubulin ligands involves the perturbation of microtubule dynamics during the G2/M phase of cell division and subsequent entry into apoptosis [1]. In this report, we challenge the established dogma by describing a unique mechanism of action caused by a novel series of tubulin ligands, halogenated derivatives of acetamido benzoyl ethyl ester. We have developed a suicide ligand for tubulin, which covalently attaches to the target and shows potent cancericidal activity in tissue culture assays and in animal tumor models. These compounds target early S-phase at the G1/S transition rather than the G2/M phase and mitotic arrest. Bcl-2 phosphorylation, a marker of mitotic microtubule inhibition by other tubulin ligands was dramatically altered, phosphorylation was rapid and biphasic rather than a slow linear event. The halogenated ethyl ester series of derivatives thus constitute a unique set of tubulin ligands which induce a novel mechanism of apoptosis.**

**Keywords:** tubulin, novel, apoptosis, anti-tumor, anti-cancer.

## Introduction

Tubulin and microtubules are important targets for anti-cancer drug development. The first FDA-approved anti-cancer tubulin ligands were the vinca alkaloids which showed therapeutic potential against lymphoma and leukemia [1,2]. The vinca alkaloids appear to target tubulin and microtubules because of their specificity measured in biochemical assays [3,4] and their affects on microtubule structure *in vivo* [5,6]. Vinca alkaloids are known to depolymerize microtubules *in vitro*. In contrast, paclitaxel stabilizes microtubules *in vitro* and *in vivo* [7,8]. Paclitaxel was recently approved for the treatment of ovarian and breast cancer [9,10]. The presently accepted mechanism of action is that all anti-tumor tubulin ligands affect dynamic microtubule structures which are most sensitive during mitosis [1,11]. Subsequent arrest at mitosis induces the apoptotic mechanism to cause cell death. We had been studying small-molecular weight compounds that interact with tubulin and require straightforward synthesis with a view to develop them as anti-cancer agents [12,13]. This article describes the novel finding that the haloacetamido benzoyl ethyl ester (HAABE derivatives, Figure 1*A*) are acting with tubulin and that these tubulin ligands can uniquely arrest cancer cells in the G1/S cell cycle transition. Optimization of the HAABE series of compounds resulted in iodine acetamido benzoyl ethyl acetate (IAABE, an iodine derivative) which has a high therapeutic potential for a variety of cancer types.

## Methods

### *Cell Culture*

All cell lines were obtained from the American Type Culture Collection (Rockville, MD) except human SP cells which were isolated from a biphenotypic leukemic cell line [34,35]. CEM cells were cultured in Iscove's Dulbecco's medium with 10% fetal calf serum (FCS), penicillin and streptomycin (250 unit/ml each). SP cells were cultured in minimal Eagle's medium with 10% FBS. Daudi, DND-1A, 786-O, MCF-7, NCI-H521 and HCT-116 cell lines were cultivated in RPMI 1640 plus 10% FBS. PBLs were cultured in RPMI 1640 plus 10% homologous plasma. All cell lines were cultured in a humid chamber at 37°C with 5% $CO_2$.

### *FACS Analysis*

DNA content was measured using a Cycle TEST kit (Becton Dickinson, San Jose, CA). Light scattering and DNA luminescence were measured with a FACScan flow cytometer (Becton Dickinson) and software Cellfit and Cell Quest (Becton Dickinson). Approximately 1000 to 5000 cells were counted from a preparation of $1\times10^6$ cells.

### *Microtubule Polymerization Assays*

The CytoDYNAMIX™ Screen 01 (Cytoskeleton Inc., Denver, CO) was used to measure microtubule polymeriza-

Abbreviations: HAABE, halogenated derivatives of acetamido benzoyl ethyl ester (halogens F, Cl, Br and I); HAABU, halogenated derivatives of acetamido benzoyl urea.

Address all correspondence to: Dr. J. George Bekesi, T.J. Martell Laboratory for Leukemia, Cancer and AIDS Research, Mount Sinai School of Medicine, New York, NY 10029.

[1]This work was supported by a Small Business Innovative Research award from the National Institutes of Health, NIGMS, Bethesda, MD, USA (A.S.D., K.M.M.) and by the TJ Martell Memorial Foundation for Leukemia, Cancer and AIDS Research in the Division of Neoplastic Diseases, Mount Sinai Medical School, New York, NY 10029 (J.D.J., J.G.B.).

[2]These authors contributed equally to this work.

Received 20 August 1999; Accepted 7 September 1999.

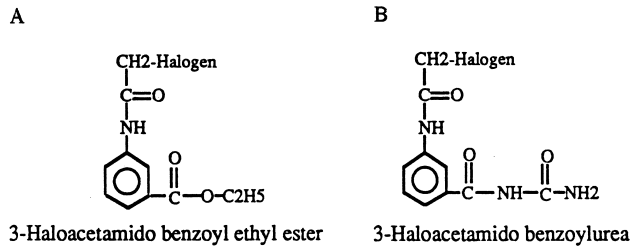


**Figure 1.** *Core structure of compounds. Structure of HAABE (A) and HAABU (B) (Halogen = F, Cl, Br, I).*

tion. The compounds were pipetted directly into each well of the 96-well plate placed on ice and using G-PEM buffer as diluent (80 mM PIPES pH 6.9, 1 mM $MgCl_2$, 1 mM EGTA, 1 mM GTP). Each well contains G-PEM buffer, compound at the concentration stated and MAP-rich tubulin at a concentration of 1 mg/ml. The plate is shaken orbitally for 20 seconds, warmed to 24°C and the absorbance is read at 340 nm once every minute for 60 minutes. The tubulin is highly purified >99% MAP-rich tubulin with a high biological activity, i.e., dynamic activity, which achieves >90% polymerization at 1.0 mg/ml [36]. Previous assays [12] were performed using impure, low-activity tubulin from Sigma Chemical Co. (St. Louis, MO) which is approximately 50% pure and has less than 20% polymerization activity [36].

*Tubulin Labeling*

Tritium-labeled IAABE was produced by Moraveck Biochemical Inc. (Brea, CA) to a specific activity of 25.5 Ci/mM. Pure tubulin (TL238; Cytoskeleton Inc.) at 3 mg/ml in 5% glycerol–G-PEM was incubated with 5 $\mu$M tritiated IAABE for 60 minutes at 37°C. The control reaction tubulin and buffer reached a maximum $OD_{340nm}$ of 0.30 over 30 minutes. The labeling reaction OD never raised above $OD_{340nm}$ of 0.01. Cellular tubulin labeling experiments were performed the same as for cytotoxicity assays except 9 cm petri dishes were used and tritium IAABE was substituted for IAABE. Cells were removed from the culture dish with trypsin EDTA treatment and were centrifuged for 2 minutes at 2000×*g*. Cell pellets were lysed in 1×sodium dodecyl sulfate (SDS) gel loading buffer containing 100 mM beta-mercaptoethanol, 1% SDS, 10% glycerol and 0.01% bromophenol blue. Pure tubulin and cell extracts were run on a 10% polyacrylamide gel and blotted onto nylon-reinforced nitrocellulose membranes. Slices of the membranes were dissected and the radioactivity counted. Molecular weight was determined by comparison with colored molecular weight markers (Novex Inc.).

Labeled tubulin for pinocytosis cell loading studies was produced as described above for radiolabeled tubulin, except non-tritiated IAABE was used at a concentration of 30 $\mu$M. The reaction products were then passed over a 30 cm G25 Sephadex column (Pharmacia Inc.) in G-PEM buffer, concentrated to 7.5 mg/ml and stored at −70°C. This removed all unbound IAABE and left pure tubulin drug covalent complex (TDCC).

*Immunofluorescence Staining of Microtubule Structure*

CEM cells incubated in the presence or absence of IAABE were collected and centrifuged in Cytospin at 700×*g* for 5 minutes. The slides were air-dried and fixed with methanol at −20°C for 20 minutes. The slides were incubated in phosphate-buffered saline (PBS) containing 1% bovine serum albumin (BSA) at 37°C for 30 minutes. After washing with PBS for 3 minutes, cells on the slides were covered with 30 $\mu$l of antihuman beta-tubulin monoclonal antibody (4 $\mu$g/ml; Accurate Antibody, Westbury, NY) and placed in a humid chamber at 24°C for 60 minutes. The slides were washed with PBS three times for 3 minutes each, followed by staining with 10 $\mu$l of fluorescein isothiocyanate (FITC)-labeled goat anti-mouse antibody (Coulter, Hialeah, FL) in a humid chamber at 24°C for 60 minutes. After washing in PBS, the stained cells were visualized under a fluorescence microscope (model MC63; Zeiss, Jena, Germany).

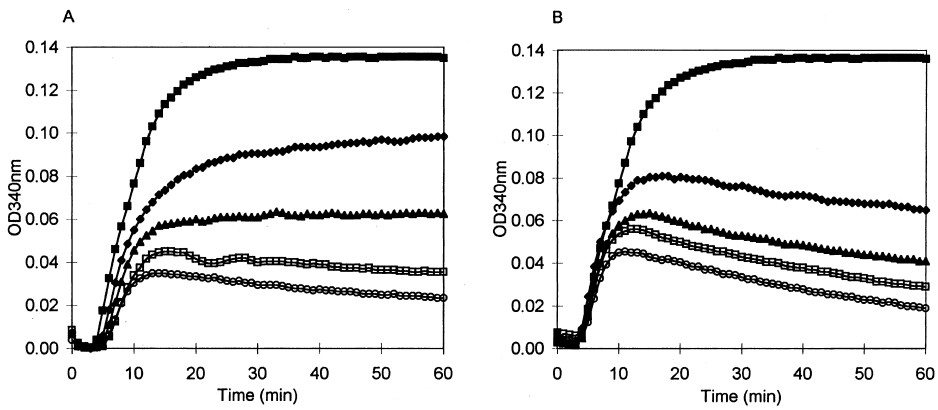


**Figure 2.** *Microtubule polymerization inhibition by IAABE and BAABE. Compounds were dissolved in G-PEM buffer at 4°C before resuspending the lyophilized tubulin in the wells of a 96-well plate (CytoDYNAMIX® Screen 01; Cytoskeleton Inc.). Absorbance was measured over time; absorbance is proportional to microtubule content. $IC_{50}$ values were determined by linear regression analysis of concentration versus percentage inhibition; concentration at 50% inhibition at 60 minutes was defined as the $IC_{50}$. Concentrations of IAABE (A) were 0 (■), 1.0 (◆), 2.5 (▲), 5.0 (□) and 10 $\mu$M (○). Concentrations of BAABE (B) were 0 (■), 10 (◆), 20 (▲), 40 (□) and 80 $\mu$M (○).*

**Table 1.** Activity of the Halogenated Acetamido Benzoyl Ethyl Ester F, Cl, Br and I Series on Microtubule Polymerization and Cancer Cell Cytotoxicity.

| Halogen | MW | Microtubule Assembly, $IC_{50}$ ($\mu$M) | Cancer Cell Cytotoxicity, $ID_{50}$ ($\mu$M) |
|---|---|---|---|
| F | 233 | >100 | >79 |
| Cl | 241 | >100 | 7.7±0.6 |
| Br | 253 | 10±1.5 | 1.9±0.2 |
| I | 271 | 2.5±0.15 | 0.17±0.03 |

NOTE. MW, molecular weight in daltons; $IC_{50}$, concentration for 50% inhibition of microtubule polymerization; $ID_{50}$, concentration for 50% cell death of CEM cancer cells.

*Apoptotic DNA Analysis*

Soluble DNA from cells was extracted treating cells in lysis buffer (10 mM Tris-HCl pH 8.0, 10 mM NaCl, 10 mM EDTA, 5% SDS) containing 1 $\mu$g/ml Proteinase-K for 1 hour at 50°C. The mixture was extracted with phenol/chloroform and precipitated with 70% ethanol and pelleted by centrifugation 14,000×*g* for 10 minutes. The pellet was dried and resuspended in $dH_2O$, the $OD_{260}/OD_{280}$ was >2.0, and the samples were treated with RNAse 100 ng/ml for 20 minutes at 37°C before running on 1% agarose gels in 1×TBE. DNA ladders were stained with 100 ng/ml ethidium bromide and visualized under UV light.

*DNA Synthesis Measurement*

CEM cells at $2\times10^5$/ml were incubated with $ID_{90}$ concentration of the compound and $^3$H-thymidine (4 $\mu$Ci/ml). Cells were harvested by vacuum filtration and filters were counted in scintillation fluid.

*Bcl-2 Analysis*

Cells were treated with different concentrations of drugs for the time range between 0 and 24 hours. Aliquots of cells were lysed in 50 mM Tris-HCl pH 7.4, 0.1% Triton X-100, 1% SDS, 250 mM NaCl, 15 mM $MgCl_2$, 1 mM DTT, 2 mM EDTA, 2 mM EGTA, 25 mM NaF, 1 mM PMSF 10 $\mu$g/ml leupeptin and 10 $\mu$g/ml aprotinin. The protein concentration was determined by a DC protein assay kit (Biorad). Equal amounts of protein were subjected to electrophoresis in 0.1% SDS and 10% polyacrylamide gels. Proteins were blotted onto nitrocellulose and blocked with 5% non-fat milk in TBST buffer. Bcl-2 was detected by probing with bcl-2 monoclonal antibody (mAb) from Pharmingen, San Diego, CA.

*Mitochondrial Permeability Transition Assay*

The method of Constantini *et al.* [21] was used to measure mitochondrial permeability transition. Briefly, mitochondria were isolated from liver by homogenization in ice-cold homogenization buffer (0.25 M sucrose, 10 mM Tris-HCl pH 7.4, 0.1 mM EGTA). Unbroken cells and cell debris were removed by centrifugation at 650×*g* for 10 minutes. Mitochondria were pelleted by centrifugation at 8000×*g* for 10 minutes, and washed twice by resuspension in homogenization buffer and centrifugation at 8000×*g* for 10 minutes. Mitochondria were diluted to 0.5 mg/ml protein in swelling buffer (0.20 M sucrose, 10 mM Tris-MOPS pH 7.4, 5 mM Tris-succinate, 1 mM Tris-phosphate, 10 $\mu$M Tris-EGTA, 2 $\mu$M rotenone). Calcium chloride 15 $\mu$M was used to sensitize the permeability pore complex. Mitochondria in swelling buffer were

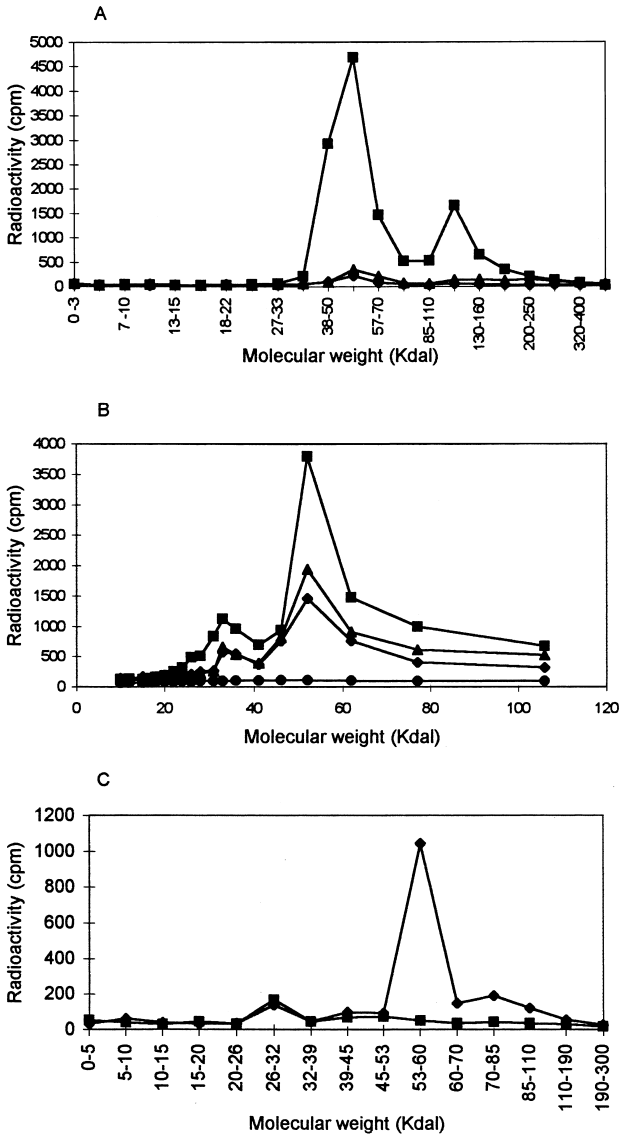


**Figure 3.** *Covalent modification of tubulin by IAABE. (A) Tubulin or BSA were incubated in the presence of $^3$H-IAABE for 0 (▲ tubulin) or 60 minutes (■ tubulin; ◆ BSA). Samples were separated on a polyacrylamide gel and blotted onto a nitrocellulose membrane. Lanes were dissected into slices and counted for radioactivity. Tubulin has a molecular weight of 55 kDa and BSA 68 kDa. The peak at 55 kDa is monomeric tubulin and the peak at 120 kDa represents tubulin dimers. (B) CEM cells were incubated in the presence of 0.37 $\mu$M $^3$H-IAABE for 0 (●), 1 (■), 4 (▲) and 12 hours (◆). Cells were harvested and lysed directly into gel loading buffer. Samples were separated on a polyacrylamide gel and blotted onto a nitrocellulose membrane. Lanes were dissected into slices and counted for radioactivity. Note major peak at 55 kDa. (C) DEAE purification of $^3$H-IAABE-labeled tubulin from CEM cells. Extracts from $^3$H-IAABE-treated cells (1 hour incubation) were purified with the DEAE method. Bound tubulin (◆) and unbound fractions (■) were blotted and counted as described above. Note that 95% of radioactivity co-eluted with the tubulin.*

pipetted into the same buffer containing the compound of interest. Absorbance was measured over 20 minutes at $OD_{540\ nm}$; absorbance is inversely proportional to swelling extent.

*Cell Loading Studies*

The method of Okada and Rechsteiner [25] was used to load CEM cells with tubulin or TDCC using the Influx™ Pinocytic Cell Loading Reagent (Molecular Probes Inc., Portland, OR). Briefly, $4\times10^6$ cells were incubated in 20 $\mu$l of hypertonic loading medium plus 20 $\mu$l of tubulin or TDCC at 7.5 mg/ml protein for 10 minutes at 37°C, followed by adding 1 ml of hypotonic lysis medium for 1.5 minutes at 37°C. Cells were finally incubated in 16 ml of normal tissue culture medium. Samples were then processed for FACS analysis.

*Cytotoxicity Assays*

Cells in suspension were seeded into 96-well plates at $10^5$cells/well, and the compounds added, total well volume was 250 $\mu$l. Cells were cultured for 48 hours and the viability was measured by trypan blue exclusion. $ID_{50}$ and $ID_{90}$ values were determined by the concentration of compound required to induce cell death in 50% or 90% of cells, respectively.

## Results

We had previously shown that the HAABU series of compounds (Figure 1*B*), strongly inhibited microtubule polymerization [12,13]; however, our initial examination of the closely related HAABE compounds showed no effects on microtubules [12]. Therefore, we decided to repeat the microtubule polymerization study using an optimized assay

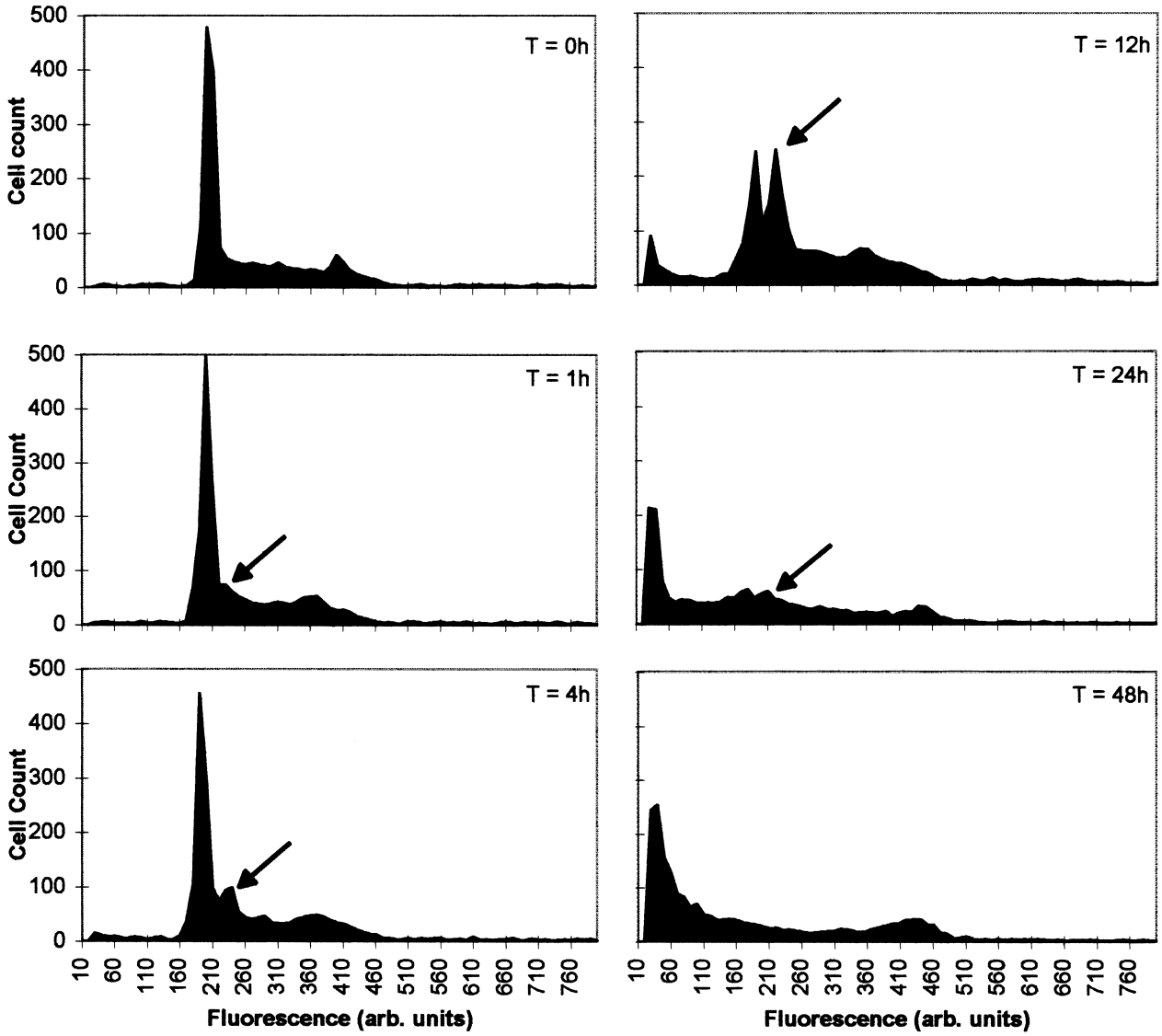


**Figure 4.** *Cell cycle arrest at G1/S transition in CEM cells treated with IAABE. CEM cells were seeded at $2\times10^5$/ml cells/ml in the presence of IAABE at the $ID_{90}$ concentration 0.37 $\mu$M. After 0, 1, 4, 12, 24 and 48 hours, samples were harvested and stained for DNA content (see Methods section) before FACS analysis. Experiments were performed twice with similar results. Approximately 1000 to 5000 cells were counted per sample. Note the peak at 2.3n DNA (arrow) in the IAABE-treated cells only.*

procedure. The CytoDYNAMIX™ Screen system (Cytoskeleton Inc.; see Methods section) was used to test activity of these derivatives against tubulin polymerization. Using this system, we detected significant microtubule inhibition with two of the HAABE compounds (BAABE and IAABE; Figure 2, *A* and *B*). There was a proportional relationship between the size of the halogen and inhibition of microtubule assembly (Table 1). The derivatives with the smallest halogens, fluorine and chlorine, did not inhibit microtubule assembly when present at 100 $\mu$M whereas the bromine and iodine derivatives had $IC_{50}$ values of 30 and 2.5 $\mu$M, respectively. One peculiarity of the microtubule inhibition activity was a decline in polymerization after a short time in the presence of compound. In particular, BAABE and IAABE showed this response (see Figure 2, *A* and *B* at >15 minutes). It was hypothesized that this effect could be due to increased GTPase activity, polymer binding activity, slow binding kinetics, or by nucleophilic attack causing a covalent modification of monomeric tubulin as would be expected by the more reactive bromine and iodine derivatives. Subsequent experiment showed the latter hypothesis to be correct.

IAABE was labeled with tritium and incubated with either pure tubulin or pure BSA. Highly specific labeling was found to be associated with tubulin, whereas BSA did not label in the same assay (Figure 3*A*). The stoichiometry of tritium-labeled IAABE binding to tubulin was found to be 0.05:1.0 (IAABE:tubulin), this value is probably an underestimate due to quenching of tritium signal by the filter; also, competitive assays with colchicine binding showed a stoichiometry binding of 0.5:1.0 which indicates that a higher stoichiometry is possible. Tritium-labeled IAABE was also used to label cellular proteins by incubating with tissue culture cells. Figure 3*B* shows that the label was rapidly incorporated (less than 1 hour) into protein with a molecular weight of 55 kDa which corresponds to the molecular weight of tubulin monomer. The amount of labeling subsequently declined over time probably because of protein metabolism and apoptosis-associated proteolysis. We determined that IAABE was binding to tubulin in cells by purifying cellular tubulin with DEAE anionic exchange resin as previously used for determining vinblastine and colchicine binding to tubulin in cellular extracts [3,4]. We found that 95% of the tritium

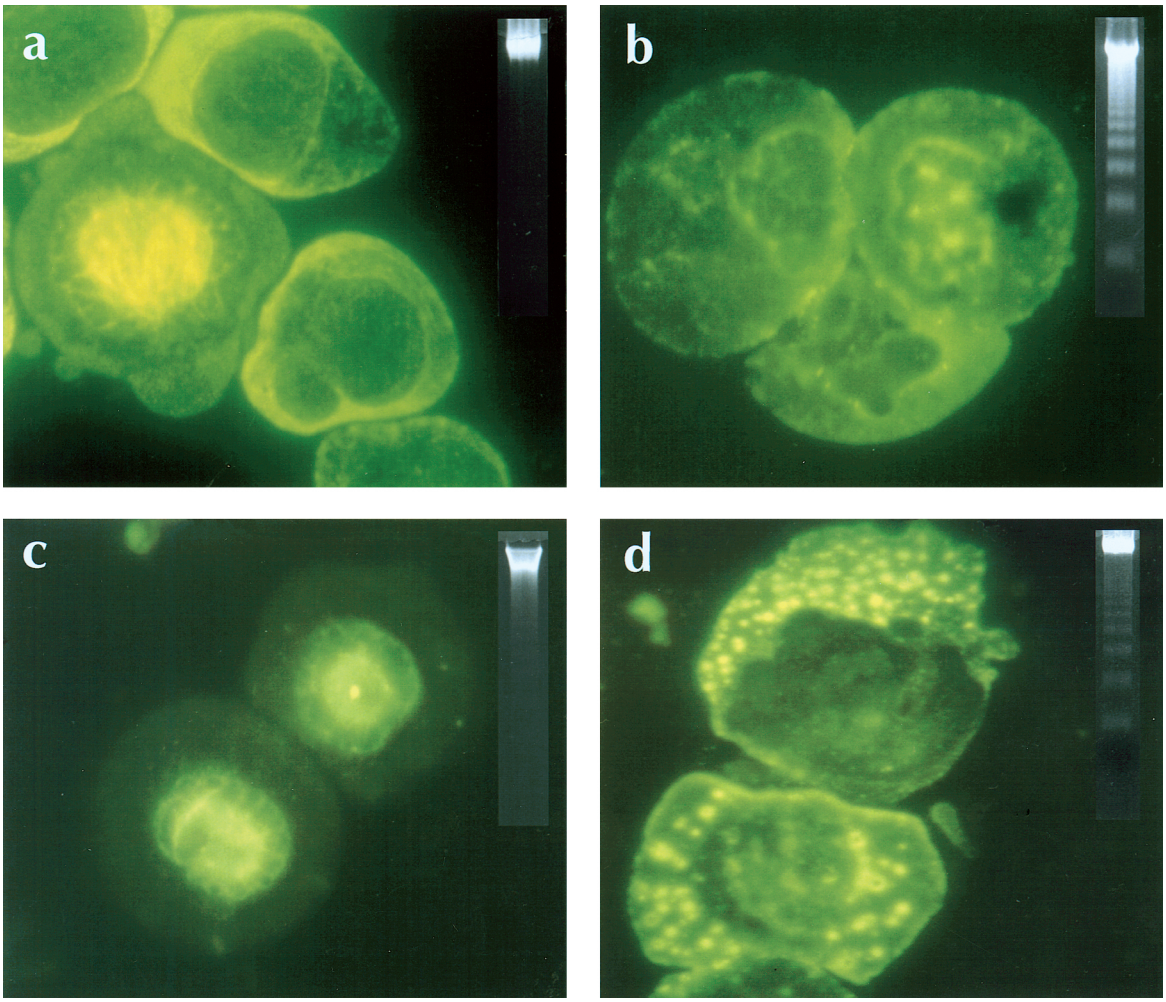


**Figure 5.** *Interferences with the formation of microtubule structure in IAABE-treated CEM cells. All cells were treated with $ID_{90}$ concentration of compounds for 12 hours [12,13]. (a) Untreated control cells, (b) IAABE, (c) paclitaxel and (d) vinblastine. Insert is a DNA extracted from the same samples run on 1% agarose gels and stained with ethidium bromide. Note absence of microtubule structure and appearance of apoptotic nuclei in IAABE-treated cells. Note strong signal of apoptotic DNA ladder in IAABE-treated cells compared to vinblastine and paclitaxel samples.*

label in the 55 kDa area of the gel was co-eluted with the purified tubulin (Figure 3*C*). These assays show that the majority of IAABE specifically labels tubulin and that tubulin is most likely the intracellular target. It is possible that cysteine is the modified amino acid because first, *in vitro*, the polymerization inhibition by IAABE is reduced in the presence of reducing agents (dithiothreitol and beta-mercaptoethanol, data reported elsewhere) and second, the compound competes for the colchicine binding site (reported elsewhere) which is associated with cysteine residues [14].

The cell cycle was analyzed by flow cytometry of propidium iodide-stained cells, IAABE (iodine derivative)-treated cells began to show an elevated S-phase within 1 hour of treatment. After 4 hours, a sharp peak emerged in early S-phase at the G1/S transition, which contained approximately 2.3n DNA (Figure 4). The new peak became dominant in this cell population at 12 hours. At this point, less than 1.0n DNA was detected indicating DNA fragmentation. A slight G2/M elevation was also seen with IAABE over the time course of the experiment, but this was much less significant than that of early S-phase block. These responses are unique among tubulin ligands which usually arrest cells in G2/M phase [1]. These responses differ from that of the HAABUs, vinblastine and paclitaxel, which cause cells to arrest characteristically in G2/M phase (4n DNA), only later (>12 hours) does the cell enter apoptosis [13,15,16]. Biochemically, the IAABE-treated cells were undergoing apoptosis with caspase pathway activation as early as the first hour of treatment (data reported elsewhere). In Figure 4, the emergence of <2.0n fragmented DNA follows after the 2.3n arrest, the G2/M peak does not alter in height and is still present at *T* = 48 hours. This strongly suggests that the 2.3n arrest is before the emergence of fragmented DNA and hence before apoptosis.

To investigate the mode of cell death, we studied key diagnostic markers of apoptosis. The HAABU derivatives were shown to cause apoptosis by phenotypic observation, DNA fragmentation and bcl-2 phosphorylation [12,13] by a similar mechanism of known tubulin ligands such as paclitaxel and vinblastine [15–17]. However, this was not the case with the HAABE derivatives. These compounds showed a unique mode of apoptosis.

First, incubating cancer cells in the $ID_{90}$ concentration of IAABE shows absence of microtubule structures, the presence of nuclear apoptotic bodies, and DNA fragmentation occurred within 6 hours. In contrast, paclitaxel shows dense mitotic spindle staining and vinblastine shows punctated aggregates of tubulin, and both showed apoptotic DNA only after 12 hours (Figure 5).

Second, in support of a novel apoptosis induction, we observed a unique time-dependent profile of bcl-2 phosphorylation. Bcl-2 phosphorylation is associated with the activity of tubulin ligands. Raf1 kinase receives an unknown signal from the tubulin/microtubule cytoskeleton which induces it to phosphorylate bcl-2 [18]. Bcl-2 is usually bound to the permeability transition pore complex of the mitochondria which suppresses pore opening and hence suppresses spontaneous apoptosis [19,20]. Phosphorylated bcl-2 disrupts bax association thus causing an increased likelihood of apoptosis [15,18]. Normally, tubulin ligands increase the amount of phosphorylated bcl-2 only after 6 hours. After this time point, the amount of phosphorylated form increases linearly over time ([17]; Figure 6*A*); however, the IAABE derivative causes a

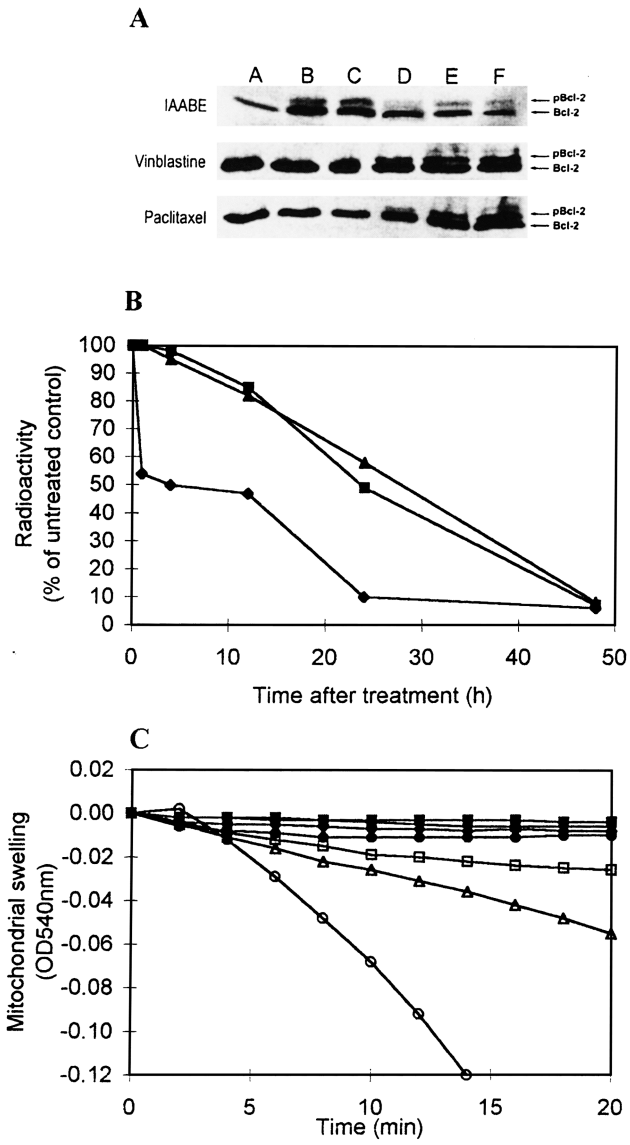


**Figure 6.** *The mode of cell death caused by IAABE. (A) Analysis of Bcl-2 phosphorylation in CEM cells treated with IAABE, vinblastine or paclitaxel ($ID_{90}$ concentration of compounds) for 0, 1, 3, 6, 12 and 24 hours (A, B, C, D, E and F, respectively) [13]. Note rapid appearance of phosphorylated bcl-2 (pBcl-2) in the IAABE samples. (B) DNA synthesis inhibition determined by $^3H$-thymidine uptake measurements. Cells were incubated with $ID_{90}$ of the compound [25]. (■) Vinblastine; (▲) BAABU; (◆) IAABE. Note that IAABE-treated cells shut down DNA synthesis very soon after drug application compared to BAABU and vinblastine which have a slow linear decrease in thymidine incorporation. (C) Effect of paclitaxel and IAABE on mitochondrial permeability transition. Mitochondria were incubated at 24°C in 15 μM $CaCl_2$ in the presence of paclitaxel or IAABE [30]. Concentration of paclitaxel were 0 (■), 5 (●), 10 (□), 20 (△) and 40 μM (○). Concentrations of IAABE were 0 (■) and 1 mM (◆). Absorbance is inversely proportional to mitochondrial swelling.*

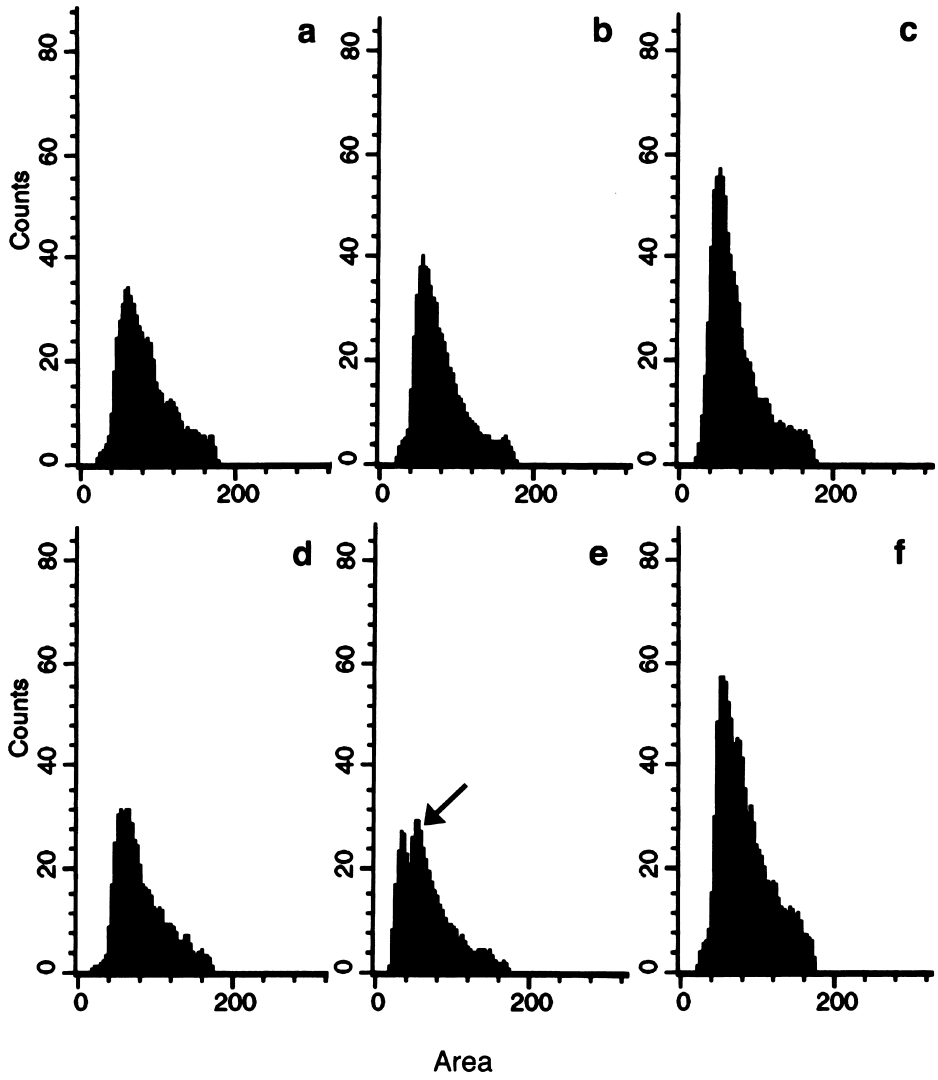


**Figure 7.** *Effects of TDCC on the cell cycle. CEM cells were loaded with tubulin or TDCC by pinocytosis. T = 1, 4 and 12 hours for tubulin only, a, b and c, respectively. T = 1, 4 and 12 hours for TDCC, d, e and f, respectively. The experiment was performed twice with similar results. Approximately 1000 to 5000 cells were counted per sample. Note the peak at 2.3n DNA (arrow) in the TDCC sample only.*

biphasic response where the initial phosphorylation is very rapid (see 1 hour time point, Figure 6*A*). After 3 hours, the relative proportion of phosphorylated bcl-2 then decreases with respect to the non-phosphorylated form; after 9 hours, the trend returns to a high ratio of phosphorylated bcl-2 at which point apoptosis is already occurring. It appears that the rapid uptake of IAABE and labeling of tubulin within an hour (Figure 3*B*) cause a rapid response in cell signaling pathways, which results in induction of apoptosis before mitotic block.

Third, using the $^{3}$H-thymidine incorporation assay, we found that cellular DNA synthesis was shut down immediately after the treatment with IAABE (Figure 6*B*), in agreement with the rapid appearance of early S-phase block induced by IAABE (Figure 2). The kinetic profile of $^{3}$H-thymidine-uptake of IAABE was remarkably different from those of vinblastine and BAABU (Figure 6*B*), which caused a significant inhibition of DNA synthesis only after M-phase arrest, i.e., greater than 12 hours.

**Table 2.** Cytotoxicity of IAABE against Different Tumor Cells.

| Human Tissue Type | Cell Line | Cytotoxicity ($\mu$g/ml) | |
|---|---|---|---|
| | | $ID_{50}$ | $ID_{90}$ |
| T-cell leukemia | CEM | 0.047 ± 0.011 | 0.1 ± 0.007 |
| Myelodysplasia syndromes | Sp | 0.085 ± 0.02 | 0.25 ± 0.02 |
| Melanoma | DND-1A | 0.25 ± 0.08 | 0.51 ± 0.04 |
| Renal cancer | 786-0 | 0.042 ± 0.006 | 0.08 ± 0.01 |
| Breast cancer | MCF-7 | 0.12 ± 0.02 | 0.49 ± 0.05 |
| Non-small cell lung cancer | NCI-H522 | 0.05 ± 0.01 | 0.09 ± 0.01 |
| Colon cancer | HCT-116 | 0.09 ± 0.02 | 0.41 ± 0.05 |
| Lymphoma | Daudi/wt* | 0.007 ± 0.001 | 0.05 ± 0.025 |
| Lymphoma | Daudi/MDR* | 0.005 ± 0.001 | 0.06 ± 0.004 |
| Normal lymphocytes | PHA stimulated† | 2.5 ± 0.3 | 5.5 ± 0.6 |

*Daudi/MDR are PGP(+) cells, and Daudi/wt are PGP(−) cells [13].
†Normal human lymphocytes were pretreated with 1 $\mu$g/ml phytohemagglutinin for 24 hours at 37°C to induce proliferation.
NOTE. $ID_{50}$ and $ID_{90}$, see Table 1 for definitions, and Refs. [12,13,42,43] for cell line origins.

**Table 3.** Murine Lymphoma Inhibition by BAABE.

| Tumor* | Treatment | No. of Mice | Therapeutic Regime | Tumor-Bearing Mice† (Tumor Volume†) | Tumor-Free Mice† |
|---|---|---|---|---|---|
| Murine EL4 lymphoma (s.c. implant) | Solvent | 15 | s.c. injection on days 4, 6, 8, 11, 13 | 15 (2731 ± 807) | 0 |
| Murine EL4 lymphoma (s.c. implant) | BAABE | 15 | s.c. injection on days 4, 6, 8, 11, 13 | 3 (1064 ± 411) | 12 |

*Murine EL4 lymphoma was implanted (s.c.) into C57 mice.
†Tumor volume was determined at $T$ = 35 days using the formula: $w^2L(\mathrm{Pi}/6)$; $w$ = width, $L$ = length and Pi = 3.142.

Fourth, the mode of cell death was further compared with that of paclitaxel by an assay to determine mitochondrial targeting [21], a key interface of the apoptotic process [22,23]. Paclitaxel is known to increase the permeability of the mitochondria by interacting with a component (probably tubulin) on the outer membrane with a $K_d$ of 5 to 20 $\mu$M [24]. This process can be measured by following the absorbance change at 540 nm associated with mitochondrial swelling (Figure 6*C*). However, the HAABE derivatives did not induce this swelling reaction even in the presence of 1.0 mM IAABE (Figure 6*C*), or in combination with tubulin and TDCCs (data reported elsewhere). This was not due to the HAABE derivatives not interacting with tubulin because the tubulin in the outer membrane of mitochondria was shown to be covalently labeled by the same method described in Figure 4*B* (data not shown). These results further underline the differences between the mechanism of action of known tubulin ligands and the HAABE derivatives.

Our data suggest a novel mechanism of action for a tubulin ligand; however, we needed to determine whether tubulin was the primary target of IAABE. Therefore, we tested whether the TDCC could cause the same cellular response as the compound alone. We purified the TDCC and introduced it into tumor cells by pinocytosis [25]. Control cells (tubulin alone) had a rapid reduction in the G0/G1 population from 25% to 15%; also the G2/M population was relatively low which can be expected after the harsh treatment with osmotic modifying solutions (Figure 7, *a* – *c*). In contrast, TDCC caused the cell cycle to arrest with 2.3n DNA (Figure 7*e*) and a concomitant decrease in the G0/G1 population as determined by the reduced peak at 2.0 nDNA. Cells arrested with 2.3n DNA are unique to IAABE-treated cells (we suggest to call it T2.3n arrest point or checkpoint), thus we attribute the difference in DNA content profiles to the presence of the complex rather than tubulin alone. The arrested cells in this case did not enter apoptosis within the period of the experiment, probably because the amount of TDCC was limited and could be metabolized by the cells' proteolytic machinery (see Figure 3*B*, reduction of tubulin label over time). The arrest at G1/S is indicative of the same effect as IAABE alone (Figure 4) indicating that TDCC can induce the same cell cycle arrest as externally administered IAABE. These data strongly suggest that the primary target of IAABE-induced apoptosis is the tubulin molecule.

Growth inhibition assays were used to determine the anti-cancer activity in tissue culture (Tables 1 and 2) and in animal models. Using CEM leukemic cells, the fluorine derivative did not inhibit tumor cell growth at 79 $\mu$M, whereas the chlorine, bromine and iodine derivative had $ID_{50}$ values of 7.7 ± 0.6, 1.9 ± 0.2 and 0.17 ± 0.03, respectively. IAABE caused a rapid dissipation of microtubule structures as shown by immunofluorescence staining (Figure 5). The iodine derivative had broad and potent cancericidal activity as determined by low $ID_{50}$ and $ID_{90}$ activities on multiple cell lines (Table 2). The greatest cancericidal activity was on the lymphoma cells (Daudi/wt and Daudi/MDR) where the ratio ($ID_{50}$ normal cells/$ID_{50}$ cancer cells) was up to 500. This compares favorably with vinblastine and paclitaxel which have values of 42 and 24, respectively.

Cell-mediated drug resistance from the PGP transporter was tested on the HAABE series; it was shown that PGP(−) cells were just as sensitive as PGP(+) cells (Table 2) indicating that this route of drug resistance for vinca alkaloids and paclitaxel [26,27] does not operate for the HAABE derivatives. These findings are similar to the HAABU derivatives [12,13].

In animal models of clonogenic lymphoma and prostate tumor growth, there was significant inhibition of tumor development (Tables 3 and 4). The bromine derivative (BAABE) rendered 80% of EL4 lymphoma-implanted mice free of the tumors, compared to all untreated controls which showed large tumor burden under the skin ($n$ = 15). In human prostate models, the iodine derivative (IAABE) showed equivalent tumor inhibition in the short-term compared to paclitaxel or vinblastine (see TI% column, Table 4). In addition, at prolonged times after treatment (90 days), we found that 20% of mice were tumor-free with IAABE treatment. Paclitaxel and vinblastine produced no tumor-free mice under similar conditions (Table 4).

**Table 4.** Prostate Carcinoma Inhibition by IAABE.

| Compound | Dose (mg/kg) | Treatment Schedule | TI% | TF/T |
|---|---|---|---|---|
| Control | Diluant* | i.v. days 1, 2, 3 | 0 | 0/10 |
| 3-IAABE | 15 | i.v. daily ×4 ×2 | 43 | 0/10 |
| 3-IAABE | 25 | i.v. 1, 2, 3 | 85 | 2/10 |
| Paclitaxel | 30 | i.v. q3 ×3 | 90 | 0/10 |
| Vinblastine | 3 | i.v. q6d ×3 | 80 | 0/10 |

**N*,*N*-dimethylacetamide, propylene glycol and Tween 80 (1:2:1 v/v/v).
NOTE. (1) $2.5\times10^6$ tumor cells were injected s.c. on day 0, treatment started at day 1. (2) TI% = Tumor growth inhibition 1 week after last treatment. (3) TF/T = Tumor-free mice at day 90 after tumor implant.

## Discussion

The HAABEs, being lipophilic, are rapidly taken up by the cell (see Figure 3: 1 hour maximal tubulin labeling), where they bind to tubulin which becomes covalently modified; this has four consequences. First, all the microtubule structures are disassembled. Second, the compounds cannot exit the cell by diffusion or the multi-drug resistance P-glycoprotein pathway, as is the case with other tubulin ligands [28,29]. Third, because the compound has a very low to non-existent off-rate for dissociation, the compound has an extremely high apparent-affinity for the target protein. Fourth, the arrest at 2.3n DNA in the G1/S transition is activated causing the cells to arrest. These effects culminate in apoptosis by a pathway which phosphorylates bcl-2 and converges on the caspase system.

The work described here indicates that TDCC has a profound effect at the arrest at 2.3n DNA; our model is a checkpoint that relates information to the cell about the ratio of monomer to polymer tubulin. The presence of the TDCC causes an aberrant level of monomeric tubulin thus indicating to the cell that there is insufficient polymer for cellular processes. Presently, there is one mechanism that is known to communicate between the tubulin and downstream apoptosis systems, tubulin ligands cause raf-1 kinase to phosphorylate bcl-2 [15,18] which disrupts its association with bax, thus inducing the subsequent steps of apoptosis [22,23]. The p53-mediated G1/S checkpoint, which is targeted by DNA alkylating agents [26], is a possible connection to the arrest at 2.3n DNA because of their temporal location in the cell cycle. It is possible that S100-related proteins such as metastasin and stathmin, which are known to bind to p53 and tubulin, respectively [29,30], may relay information from the tubulin system to the p53 signaling pathway. It is known that there is cross-talk between the S100 family members in terms of expression regulation [31], i.e., downregulation in one family member causes downregulation in another. Thus sequestration of stathmin by TDCC may lead to rapidly reduced levels of the S100 pool [31], and subsequent p53 signaling pathway disruption. In this regard, paclitaxel induces a low percentage of normal cells (but not cancer cells) to arrest in the G1 phase [32], suggesting a connection between this G1 phase checkpoint and the arrest at 2.3n DNA described here.

Tubulin covalently modifying compounds have desirable characters for therapeutic candidates. For example, cells grown in low concentrations of these compounds do not develop resistance (data reported elsewhere, and Ref. [33]). Other advantages include high affinity and specificity. In addition, the HAABE derivatives differ significantly with respect to other covalently modifying tubulin ligands, especially on cancericidal index, tubulin polymerization profiles, bcl-2 inactivation, cell cycle, DNA synthesis and mitochondrial permeability transition pore complex activation. Finally, the fact that IAABE has a cancericidal index of 500 means that this compound is approaching the efficacy often associated with anti-microbial compounds. Future anti-cancer drug development programs will focus on novel mechanisms to increase potency and decrease side effects; because of their quick absorption, rapid mechanism of action and high specificity, we believe that the HAABE derivatives will fill this need.

## Acknowledgements

We thank The National Cancer Institute Developmental Screening Program for evaluating the $IC_{50}$ and $IC_{90}$ values of 786-0, MCF-7, NCI-H522 and HCT-116 cell lines, and Joshua Nelson, Andrew Kuhn, Eman Isaacks, Fo-Nian Chu and Mathew Hurley for critical analysis of experimental detail.

## References

[1] Dumontet C, and Sikic B (1999). Mechanisms of action of and resistance to anti-tubulin agents: microtubule dynamics, drug transport and cell death. Review in *J Clin Oncol* **17**, 1061–1070.

[2] Rowinsky EK, and Donehower RC (1991). The clinical pharmacology and use of anti-microtubule agents in cancer chemotherapeutics. *Pharmacol Ther* **52**, 35–84.

[3] Wilson L (1970). Properties of colchicine binding protein from chick embryo brain. Interactions with vinca alkaloids and podophyllotoxin. *Biochemistry* **9**, 4999–5007.

[4] Wilson L, Creswell CR, and Chin D (1975). The mechanism of action of vinblastine. Binding of [acetyl-3H] vinblastine to embryonic chick brain tubulin and tubulin from sea urchin sperm tail outer doublet microtubules. *Biochemistry* **14**, 5586–5592.

[5] Malawista SE, Bensch KG, and Sato H (1968). Vinblastine and griseofulvin reversibly disrupt the living mitotic spindle. *Science* **160**, 770–772.

[6] George P, Journey LJ, and Goldstein MN (1965). Effect of vincristine on the fine structure of HeLa cells during mitosis. *J Natl Cancer Inst* **35**, 355.

[7] Schiff PB, and Horwitz SB (1979). Promotion of microtubule assembly *in vitro* by taxol. *Nature* **277**, 665.

[8] Schiff PB, Fant J, and Horwitz SB (1980). Taxol stabilizes microtubules in mouse fibroblast cells. *Proc Natl Acad Sci USA* **77**, 1561.

[9] Sandercock J, Parmar MK, and Torri V (1998). First-line chemotherapy for advanced ovarian cancer: paclitaxel, cisplatin and the evidence. *Br J Cancer* **78**, 1471–1478.

[10] Miller KD, and Sledge GW, Jr (1999). Taxanes in the treatment of breast cancer: a prodigy comes of age. *Cancer Invest* **17**, 121–136.

[11] Jordan MA, and Wilson L (1998). Microtubules and actin filaments: dynamic targets for cancer chemotherapy. *Curr Opin Cell Biol* **10**, 123–130.

[12] Jiang JD, Wang Y, Roboz J, Strauchen J, Holland JF, and Bekesi JG (1998). Inhibition of microtubule assembly in tumor cells by 3-bromoacetylamino benzoylurea, a new cancericidal compound. *Cancer Res* **58**, 2126–2133.

[13] Jiang JD, Davis AS, Middleton KM, Ling Y-H, Perez-Soler R, Holland JF, and Bekesi JG (1998). 3-(Iodoacetamido)-benzoylurea: a novel cancericidal tubulin ligand that inhibits microtubule polymerization, phosphorylates bcl-2, and induces apoptosis in tumor cells. *Cancer Res* **58**, 5389–5395.

[14] Luduena RF, and Roach MC (1981). Interaction of tubulin with drugs and alkylating agents: 2. Effects of colchicine, podophyllotoxin and vinblastine on the alkylation of tubulin. *Biochemistry* **20**, 444–4450.

[15] Halder S, Chintapalli J, and Croce CM (1996). Taxol-induced bcl-2 phosphorylation and death of prostate cancer cells. *Cancer Res* **56**, 1253–1255.

[16] Ling YH, Consoli U, Tornos C, Andreeff M, Perez-Soler R (1998). Accumulation of cyclin B1, activation of cyclin B1-dependent kinase and induction of programmed cell death in human epidermoid carcinoma KB cells treated with taxol. *Int J Cancer* **75**, 925–932.

[17] Halder S, Basu A, and Croce CM (1997). Bcl-2 is the guardian of microtubule integrity. *Cancer Res* **57**, 229–233.

[18] Blagosklonny MV, *et al.* (1997). Raf1/bcl-2 phosphorylation: a step from microtubule damage to cell death. *Cancer Res* **57**, 130–135.

[19] Yang J, *et al.* (1997). Prevention of apoptosis by Bcl-2: release of cytochrome c from mitochondria blocked. *Science* **275**, 1129–1132.

[20] Kluck RM, Bossy-Wetzel E, Green DR, and Newmeyer DD (1997). The release of cytochrome c from mitochondria: a primary site for bcl-2 regulation of apoptosis. *Science* **275**, 1132–1136.
[21] Costantini P, Petronilli V, Colona R, and Bernardi P (1995). On the effects of paraquat on isolated mitochondria. Evidence that paraquat causes opening of the cyclosporin A-sensitive permeability transition pore synergistically with nitric oxide. *Toxicology* **99**, 77–88.
[22] Marchetti P, *et al.* (1996). Mitochondrial permeability transition is a central coordinating event of apoptosis. *J Exp Med* **183**, 1155–1160.
[23] Zamzami N, *et al.* (1996). Mitochondria control of nuclear apoptosis. *J Exp Med* **183**, 1533–1544.
[24] Evtodienko YV, *et al.* (1996). Microtubule-active drugs suppress the closure of the permeability transition pore in tumour mitochondria. *FEBS Lett* **393**, 86–88.
[25] Okada CY, and Rechsteiner M (1982). Introduction of macromolecules into cultured mammalian cells by osmotic lysis of pinocytic vesicles. *Cell* **29**, 33–41.
[26] Brown JM, and Wouters BG (1999). Apoptosis, p53, and tumor cell sensitivity to anticancer agents. *Cancer Res* **59**, 1391–1399.
[27] Huang Y, Ibrado AM, Reed JC, Bullock G, Ray S, Tang C, and Bhalla K (1997). Co-expression of several molecular mechanisms of multidrug resistance and their significance for paclitaxel cytotoxicity in human AML HL-60 cells. *Leukemia* **11**, 253–257.
[28] Dey S, Ramachandra M, Pastan I, Gottesman MM, and Ambudkar SV (1997). Evidence for two nonidentical drug-interaction sites in the human P-glycoprotein. *Proc Natl Acad Sci USA* **94**, 10594–10599.
[29] Parker C, Lakshmi MS, Piura B, and Sherbet GV (1994). Metastasis associated mts1 gene expression correlates with increased p53 detection in B16 murine melanoma. *DNA Cell Biol* **13**, 343–351.
[30] Marklund U, Larsson N, Gradin HM, Brattsand G, and Gullberg M (1996). Oncoprotein 18 is a phosphorylation responsive regulator of microtubule dynamics. *EMBO J* **15**, 5290–5298.
[31] Sherbet GV, and Lakshmi MS (1998). S100A4 (MTS1) calcium binding protein in cancer growth, invasion and metastasis. *Anticancer Res* **18**, 2415–2422.
[32] Trielli MO, Andreassen PR, Lacroix FB, and Margolis RL (1996). Differential taxol-dependent arrest of transformed and non-transformed cells in the G1 phase of the cell cycle, and specific-related mortality of transformed cells. *JCB* **135**, 689–700.
[33] Shan B, *et al.* (1999). Selective, covalent modification of beta-tubulin residue Cys-239 by T138067, an antitumor agent with *in vivo* efficacy against multidrug resistant tumors. *Proc Natl Acad Sci USA* **96** (10), 5686–5690.
[34] Banjeree R, *et al.* (1992). Productive non-lytic HIV-1 replication in a newly established human leukemia cell line. *Proc Natl Acad Sci USA* **89**, 996–1000.
[35] Bekesi JG, *et al.* (1995). Translocation of cytoplasmic antigen markers in a biphenotypic cell line derived from a patient with myelodysplasia syndrome. *Mol Cell Differ* **3**, 111–123.
[36] Davis AS, and Middleton KM (1998). Lyophilized tubulins. USPTO application no. 09/310,981. Patent pending.